Recombinant Mammalian Tubulin Polyglutamylase TTLL7 Performs both Initiation and Elongation of Polyglutamylation on β-Tubulin through a Random Sequential Pathway†

Masahiro Mukai,‡ Koji Ikegami,‡,§ Yuki Sugiura,‡,|| Kouhei Takeshita,⊥ Atsushi Nakagawa,⊥ and Mitsutoshi Setou*,‡,§

Mitsubishi Kagaku Institute of Life Sciences (MITILS), Minamiooya, Machida, Tokyo 194-8511, Japan, Department of Molecular Anatomy, Hamamatsu University School of Medicine, 1-20-1 Handayama, Hamamatsu 431-3192, Shizuoka, Japan, Department of Bioscience and Biotechnology, Tokyo Institute of Technology, Yokohama, Kanagawa 226-8501, Japan, and Research Center for Structural and Functional Proteomics, Institute for Protein Research, Osaka University, 3-2 Yamadaoka, Suita, Osaka 565-0871, Japan

Received November 4, 2008; Revised Manuscript Received December 15, 2008

ABSTRACT: Tubulins undergo unique post-translational modifications, such as tyrosination, polyglutamylation, and polyglycylation. These modifications are performed by members of a protein family, the tubulin tyrosine ligase (TTL)-like (TTLL) family, which is characterized by the presence of a highly conserved TTL domain. We and others have recently identified tubulin polyglutamylases in the TTLL family [Janke, C., et al. (2005) *Science 308*, 1758−1762; Ikegami, K., et al. (2006) *J. Biol. Chem. 281*, 30707−30716; van Dijk, J., et al. (2007) *Mol. Cell 26*, 437−448]. Previously, we identified TTLL7 as a β-tubulin-selective polyglutamylase. However, there is controversy over whether TTLL7 functions as an initiase, elongase, or both in polyglutamylation. In this report, we investigate the polyglutamylation reaction by TTLL7 by employing a recombinant enzyme and in vitro reaction. Two-dimensional electrophoresis and tandem mass spectrometry showed that TTLL7 performed both the initiation and elongation of polyglutamylation on β-tubulin. Recombinant TTLL7 performed with a maximal and specific activity to polymerized tubulin at a neutral pH and a lower salt concentration. The initial rate and inhibitor analyses revealed that the mechanism of binding of three substrates, glutamate, ATP, and tubulin, to the enzyme was a random sequential pathway. Our findings provide evidence that mammalian TTLL7 performs both initiation and elongation in the polyglutamylation reaction on β-tubulin through a random sequential pathway.

In neuronal cells, the microtubule (MT)[1] functions as a crucial molecular railway on which molecular motors move (*1*) to deliver several important molecules such as glutamate receptors (*2, 3*) and synaptic vesicles (*4*) to appropriate places. The MT also plays pivotal roles in a variety of cellular activities, such as cell motility (*5, 6*) and cell division (*7, 8*). The diverse and specialized functions of microtubules can be attributed to the heterogeneity of tubulin and the diversity of post-translational modifications (PTMs). In fact, tubulin, especially in specialized intracellular structures such as ciliary or flagellar axonemes, neuronal processes, or centrioles, undergoes various PTMs: acetylation, phosphorylation, detyrosination/tyrosination, polyglycylation, and polyglutamylation (*9*). Evidence that those PTMs play crucial roles in MT function has accumulated. The acetylation of α-tubulin is important for long-distance trafficking mediated by the KIF5 molecular motor in axonal transport (*10*). The phosphorylation of β-tubulin accompanies neurite outgrowth and is dependent on the polymer level (*11, 12*). The detyrosination of α-tubulin increases the binding affinity of KIF5 for microtubules (*13, 14*). Tubulin polyglycylation is thought to be important for the proper construction of ciliary axonemes (*15*). Injections of antibodies specific for polyglutamylated tubulins into living cells have revealed that the modification is important for flagellar or ciliary motility (*5, 6*), and centrosome stability (*7*). The binding affinity of microtubule-associated proteins (MAPs), both structural and motor MAPs, for the MT is regulated by polyglutamylation (*16, 17*). Recently, we reported the physiological roles of the polyglutamylation of α- and β-tubulin in neurons. The α-tubulin polyglutamylation serves as a molecular "traffic sign" for targeting KIF1 kinesin to neuronal processes and is required for continuous synaptic transmission (*4*). β-Tubulin polyglutamylation regulates neuronal development (*18*).

The earliest identified enzyme for tubulin PTMs is a tyrosination-performing enzyme, tubulin tyrosine ligase

† This research was supported by the Mitsubishi Kagaku Institute of Life Science, by a WAKATE-S grant from the JSPS, and by a SENTAN grant from the JST (M.S.).

* To whom correspondence should be addressed. Phone or fax: +81-53-435-2292. E-mail: setou@hama-med.ac.jp.

‡ Mitsubishi Kagaku Institute of Life Sciences.

§ Hamamatsu University School of Medicine.

|| Tokyo Institute of Technology.

⊥ Osaka University.

[1] Abbreviations: PTM, post-translational modification; MT, microtubule; MAP, microtubule-associated protein; TTL, tubulin tyrosine ligase; TTLL, TTL-like protein; NB, newborn; AD, adult; MS, mass spectrometry.

10.1021/bi802047y CCC: $40.75
Published on Web 01/16/2009

(TTL) (*19*−*21*). TTL catalyzes the readdition of tyrosine to the C-terminus of detyrosinated α-tubulin. Recently, we and other researchers have succeeded in identifying polyglutamylation- or polyglycylation-performing enzymes, polyglutamylases or polyglycylase. Eddé and co-workers demonstrated that a polyglutamylase complex purified from the murine brain is composed of at least five components, PGs1−5, which contain a protein homologous to the TTL (*22*−*24*). The TTL-homologous protein is, thus, termed TTL-like (TTLL) 1 (*24*). TTL and TTLL proteins have a conserved TTL domain required for the enzyme reaction. The mammalian genome encodes 13 independent TTLL proteins (*24*). The TTL-homologous domain contains subdomains highly homologous to the catalytic domain conserved in a large enzyme superfamily of ADP-forming enzymes (*25, 26*) or ATP-grasp enzymes (*27*), which includes bacterial ATP-dependent amino acid ligase activities, D-Ala-D-Ala-ligase. We revealed that mammalian TTLL7 functions as a β-tubulin-selective polyglutamylase (*18*) and that the TTLL1- and PGs1-containing enzyme complex performs α-tubulin polyglutamylation in the brain (*4*). Further studies have revealed that other polyglutamylases to both α- and β-tubulin are harbored in the TTLL family (*18, 24, 28*). TTLL5, -6, -11, and -13 are identified as α-tubulin polyglutamylases, while TTLL4 is a β-tubulin polyglutamylase (*18, 28*). We have found that TTLL10 is a polyglycylase for nucleosome assembly protein 1 (NAP1) (*29*), although tubulin polyglycylases remain to be identified.

Despite such successes in identifying modification-performing enzymes, the characterization of these enzymes relies on the usage of enzymes purified from natural tissues or cell lines that ectopically overexpress enzymes. The available evidence suggests that TTLL4 and TTLL7 identified as β-tubulin polyglutamylases lack sufficient activity to elongate the polyglutamate chain; i.e., they function mainly as initiases (*28*). However, this finding is in disagreement with that showing extensive polyglutamylation of β-tubulin in the adult brain (*30*). Given the complex reaction of polyglutamylation and polyglycylation, i.e., the fact that they can be separated into two different reactions, initiation and elongation, an assay of enzyme activity should eliminate contaminating factors that are derived from original tissues or cells. Nonetheless, employing pure recombinant enzyme expressed in bacteria is limited to an investigation of substrate specificities (α- and β-tubulins, or NAP1) (*28*). In this report, we investigate the polyglutamylation steps of TTLL7 in detail by thoroughly employing a bacterially expressed recombinant protein and in vitro reaction to solve this contradiction. We present evidence that TTLL7 performs both initiation and elongation of polyglutamylation and elongates the polyglutamate chain on β-tubulin beyond the level observed in the brain through a random sequential binding mechanism for three substrates: glutamate, ATP, and MT.

EXPERIMENTAL PROCEDURES

Plasmid Construction. The plasmids containing the coding sequence of mTTLL7 were prepared as described previously (*18*). The full coding sequence from the original pFLCI vector was amplified using primers. To obtain the expression vector for the GST-fused protein, the amplified fragments were inserted into a pGEX-6p1 glutathione *S*-transferase (GST) gene fusion system (GE Biosciences) vector using appropriate restriction enzymes.

Preparation of Recombinant TTLL7. The mouse TTLL7 DNA fragment inserted into a pGEX-6p1 vector was expressed in an *Escherichia coli* Rossetta (DE3) strain (Novagen) at 26 °C and 80 rpm in a smooth flask by induction with a final isopropyl β-thiogalactopyranoside (IPTG) concentration of 0.4 mM. The harvested cells were resuspended in Tris-buffered saline (TBS) that included a protein inhibitor cocktail (Roche) and 1 mg/mL lysozyme. The cells were disrupted by sonication pulses (4−8 × 30 s) on ice using an ultrasonic processor (Tomy Seiko Ltd.). The obtained lysate was centrifuged for 50 min at 35000*g* and 4 °C. The supernatant was incubated for 3 h at 4 °C with glutathione-Sepharose 4B beads (GE Biosciences Corp.) to bind the GST fusion protein to the beads. To remove nonspecifically bound proteins, the beads were washed with TBS and PreScission cleavage buffer [50 mM Tris-HCl (pH 7.4), 20 mM NaCl, 1 mM EDTA, and 1 mM DTT]. The beads were incubated with PreScission protease at 4 °C to cut out mTTLL7 from the GST-fused form. After overnight incubation, mTTLL7 protein released into the supernatant was stored at −80 °C. Recombinant TTLL7 was stable and retained activity for at least 3 months at −80 °C. The addition of DTT to the storage solution was crucial for preserving enzyme activity. The enzyme activity was decreased by 1 order of magnitude when the enzyme was stored without DTT.

Tubulin Polyglutamylase Assay. Enzyme activity was measured by the incorporation of [^{3}H]glutamate into tubulin at pH 7.0. The reaction mixture, which contained 50 mM MES (pH 7.0), 8 mM $MgCl_2$, 2.5 mM DTT, 10 μM paclitaxel, and 0.2 mg/mL mouse tubulin, was warmed at 37 °C for 10 min to polymerize tubulin to MTs. mTTLL7, L-[^{3}H]glutamate, and 0.5 mM ATP were then added, and the mixture (10 μL) was incubated at 30 °C for 1 h for steady state reaction or 10 min for initial rate kinetic analysis. After incubation, to assess the whole incorporation of glutamate into microtubules, the mixture was directly loaded onto a GF/F glass filter and the [^{3}H]polyglutamylated MTs were precipitated on the filter with 10% trichloroacetic acid (TCA). After the sample had been washed with 5% TCA and 100% ethanol, the filter was dried and then transferred to a scintillation cocktail (OCS). To measure the radioactivity incorporated in α- and β-tubulin separately, the reaction mixture was subjected to sodium dodecyl sulfate−polyacrylamide gel electrophoresis (SDS−PAGE) using 95% pure SDS (Sigma-Aldrich), which enabled us to separate α- and β-tubulins. The separated tubulins were blotted onto a nitrocellulose membrane and visualized with Ponceau S. The amount of tritium was measured with a Winspectral 1414 liquid scintillation counter (Wallac, Turku, Finland) with accumulation for 1 min. The amino acid sequences of the β-tubulin C-terminal peptides used as inhibitors are DATAEEEGEMYEDDDEESEAQGPK (β-tub III) and DATAEEGEFEEEAEEEVA (β-tub IV).

Two-Dimensional Electrophoresis and Western Blot Analysis. Tubulin was resolved in lysis buffer [7 M urea, 2 M thiourea, 4% CHAPS, 40 mM DTT, and 2% IPG buffer (pH 4.5−5.5)]. First, isoelectric focusing was performed using the Multiphor II instrument (GE Biosciences) with an immobilized pH linear gradient gel (IPG gel) from pH 4.5

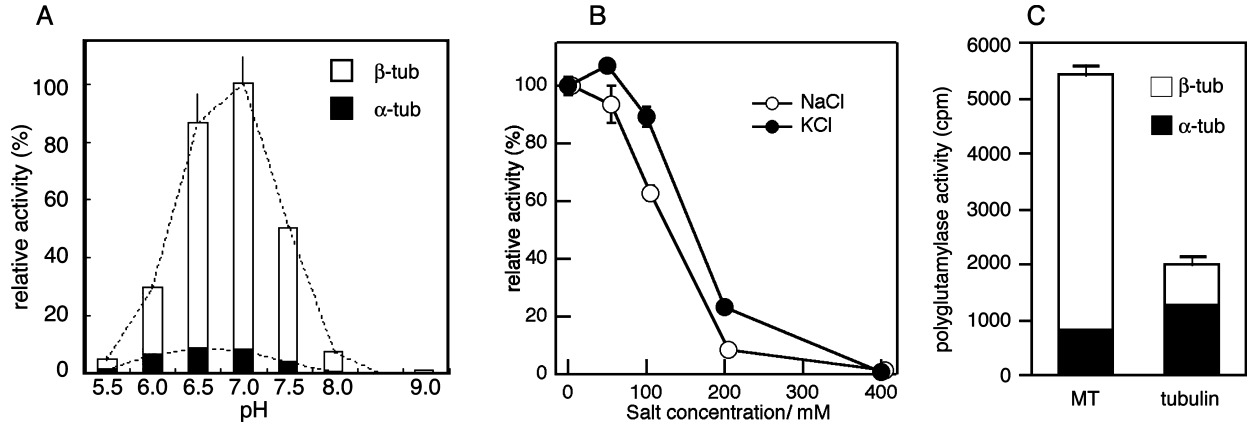

FIGURE 1: Recombinant TTLL7 shows β-tubulin polyglutamylase activity under neutral conditions. (A) pH and (B) salt dependence of polyglutamylase activity of recombinant TTLL7. (C) Reaction activities for α- and β-tubulin were dependent on tubulin polymerization.

to 5.5, 24 cm in length. Two-dimensional gel electrophoresis was carried out using a normal SDS−polyacrylamide gel. Separated tubulin spots were blotted onto PVDF membranes (Millipore). The membranes were blocked with 10% goat serum and probed with diluted primary antibodies at 4 °C overnight. The following primary antibodies were used: GT335 for polyglutamylated tubulin (*31*) at 1:20000, DM1A for α-tubulin at 1:10000, and Tub2.1 for β-tubulin at 1:2000. Binding antibodies were detected with a goat anti-mouse IgG coupled to horseradish peroxidase (1:10000) at room temperature for 1 h. The signal was visualized using an ECL kit (GE Biosciences).

Mass Spectrometry. To sufficiently polyglutamylate tubulin, purified newborn mouse tubulin was treated with TTLL7 at 37 °C for 5 h. The tubulin was separated into α- and β-tubulin by SDS−PAGE employing 95% pure SDS. The tubulin was visualized by being stained with Coomassie brilliant blue. The band corresponding to β-tubulin was excised and rinsed twice for 10 min each with 50% acetonitrile and once for 5 min with 100% acetonitrile. After the rinse, the gel was dehydrated with a SpeedVac (TeleChem International, Sunnyvale, CA) for 15 min. A volume of reduction buffer (10 mM DTT and 25 mM NH_4HCO_3) sufficient to cover the gel was added, and the gel was incubated for 1 h at 56 °C. After the gel had cooled to room temperature, the reduction buffer was replaced with alkylating buffer (55 mM iodoacetamide and 25 mM NH_4HCO_3). During alkylation, the gel was incubated at room temperature in the dark for 45 min. Next, the gel was washed with 25 mM NH_4HCO_3 once and with 50% acetonitrile twice. To facilitate absorption of digestion buffer, the gel was dehydrated using a SpeedVac and then swollen in digestion buffer (25 mM NH_4HCO_3, containing 20 μg/mL endoproteinase Asp-N) on ice. After 30 min, the supernatant was removed and incubated overnight at 37 °C. Peptide extraction was performed by incubation in 50% acetonitrile. After the extraction, the peptide extract was concentrated with the SpeedVac. We used an anion exchange tip (Nutip; Glygen, Columbia, MD) for both purification of the C-terminal end of tubulin and desalting (*4*). The wash solution consisted of 20 mM $HCOONH_4$. 1 M TFA and 10% acetonitrile was used for elution. One-half microliter of eluted peptide was applied to a MALDI plate (AnchorChip, Bruker Daltonics), and 2,5-DHB (5 mg/mL) was applied to the peptide for the formation of cocrystals. MS was performed using a MALDI time-of-flight (TOF)/TOF-type instrument (Ultraflex 2 TOF/TOF; Bruker Daltonics) as described previously (*32, 33*). This instrument was equipped with a 355 nm Nd:YAG laser. Data acquisition was performed in positive ion mode using an external calibration method.

RESULTS

Recombinant TTLL7 Has Maximal and Specific Activity for Polymerized Tubulin at Neutral pH and a Lower Salt Concentration. To investigate in detail the enzymatic properties of pure recombinant TTLL7 expressed bacterially, we first sought to determine the optimal conditions for enzyme activities. We investigated the pH dependency of the enzyme. The pH dependency of the tubulin polyglutamylase activity was measured in a range between pH 5.0 and 9.0 (Figure 1A). The enzyme activity, especially for β-tubulin, began to increase at pH 6.0−7.0, reached a peak at 7.0, and then decreased at pH >7.0 (Figure 1A).

We next examined the optimal ion strength for the TTLL7 enzyme activity. The polyglutamylase activity of recombinant TTLL7 was inhibited by NaCl in proportion to the concentrations of NaCl: 100 mM NaCl suppressed the enzyme activity at 40%, and 200 mM NaCl suppressed it at 90% (Figure 1B). One-hundred thirty millimolar was calculated as the concentration at which NaCl reduces TTLL7 activity to 50%. KCl also affected the TTLL7 enzyme activity in a manner similar to that of NaCl, although the effect was slightly weaker than that of NaCl (Figure 1B).

We investigated whether recombinant TTLL7 preferred polymerized tubulin as its substrate. The whole activity to MTs was ~2.5-fold higher than that to unpolymerized tubulin (Figure 1C). When MTs were used as substrates, recombinant TTLL7 exhibited activity highly preferential to β-tubulin (Figure 1C). The substrate preference drastically decreased when unpolymerized tubulin dimers were used as substrates (Figure 1C). This result indicates that the β-tubulin specificity of TTLL7 depends on microtubule formation. Taken together, we used the optimal conditions determined here throughout this study.

Recombinant TTLL7 Performs both the Initiation and Elongation of Polyglutamylation Steps on β-Tubulin in Vitro. Polyglutamylation can be divided into two steps, a first initiation step and a second elongation step (*31, 34*). In the initiation step, first glutamate binds to the γ-carboxy group of the tubulin main body. In the elongation step, glutamates are attached to the α-carboxy group of the branching

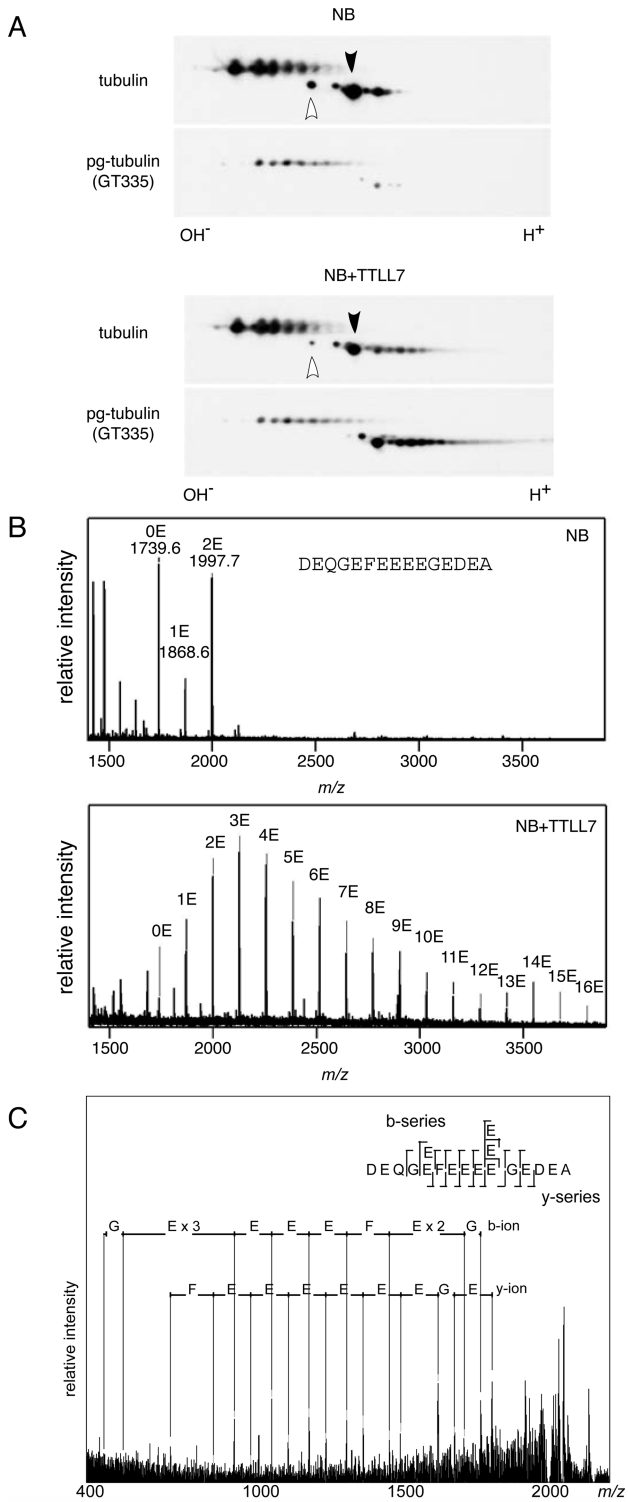

FIGURE 2: Recombinant TTLL7 performs both initiation and elongation of polyglutamylation of β-tubulin. (A) Western blot analysis of high-resolution two-dimensional electrophoresis of NB tubulin treated with recombinant TTLL7. The blot was probed in sequence with antibodies against α,β-polyglutamylated (pg) tubulin. Black and white arrowheads denote nonglutamylated β-tubulin II and III spots, respectively. (B) Mass spectra of C-terminal peptides of NB β-tubulin II (top panel) and those peptides after incubation with TTLL7 (bottom panel). The sequence of the unmodified peptide at *m/z* 1739.6 is indicated. The glutamylated peptides are marked as E1−E16 according to the number of additional glutamates. (C) Tandem mass spectrum of the parent ion signal at *m/z* 2126.7, the β-tubulin II C-terminal peptide into which three glutamates were incorporated by TTLL7 treatment (peak 3E in panel B). The sequence of the corresponding peptide, with a scheme of the y and b fragmentation series, is illustrated.

glutamate chain. Thus, the entire process of polyglutamylation may be accomplished by both an "initiase" and an "elongase" (*28*). It was reported that TTLL7 mainly functions as an initiase for β-tubulin in vivo by analyses using anti-polyglutamate antibodies, GT335 and polyE (*28*). However, it is difficult to rule out the possibility that the in vivo assay contains strong suppressors for polyglutamate chain elongation, e.g., the presence of endogenous reverse enzymes (*22*). Thus, we investigated the reaction preference of TTLL7 through the in vitro reaction employing pure recombinant enzyme.

We first performed a high-resolution two-dimensional PAGE analysis to investigate in detail whether TTLL7 can elongate the polyglutamate chain (Figure 2A). The β-tubulin of the adult mouse (AD) brain is highly glutamylated, but that of the newborn mouse (NB) is almost not glutamylated (*8, 30*). Therefore, we used NB tubulin to make it easy to detect the effect of TTLL7. The black and white arrowheads in Figure 2A denote nonglutamylated β-tubulin II and III spots, respectively. Incubation with recombinant TTLL7 drastically reduced the amount of nonglutamylated β-tubulin and produced more acidic spots, suggesting that "poly"-glutamylated β-tubulin is generated (Figure 2A).

We further investigated the length of the polyglutamate chain added by the recombinant TTLL7 incubation by means of matrix-assisted laser desorption/ionization (MALDI) mass spectrometry (MS). In newborn β-tubulin, a peptide with an ion at *m/z* 1739.6 was detected with the highest intensity (Figure 2B). The value of *m/z* was identical to that of the unmodified form of the mouse β-tubulin II C-terminus (Figure 2B). TTLL7 treatment produced many peptide peaks at even intervals with an *m/z* value of 129. The maximal *m/z* value detected was 3804, which corresponded to the C-terminus of β-tubulin II having 16 extra glutamate residues (Figure 2B). Using tandem mass spectrometry (MS^n), we identified the peptide with an ion at *m/z* 1739.6 as ^{431}DEQG**E**FEEEEGEDEA^{445} (431−445) of β-tubulin II and found that glutamylation occurred at the reported glutamylation site, E435 (*35*), and a newly identified site, E440 (Figure 2C). The detail of the identification of polyglutamylation sites is demonstrated in S1 of the Supporting Information by MS^n analysis of the standard peptide of the C-terminus of β-tubulin III that contained four extra glutamates at a reported glutamylation site (*36*). Our results indicate that recombinant TTLL7 catalyzes both the initiation and elongation steps of polyglutamylation in vitro.

Initial Rate Kinetic Analysis Reveals Sequential Substrate Binding in the TTLL7 Enzyme Reaction. Next, we investigated how TTLL7 performs its enzyme activity. To this end, we examined the kinetic analysis for the initial rate of the recombinant TTLL7 activity. All kinetic assays were performed over a 10 min interval, because the linearity of the reaction was maintained during the first 10 min by a preliminary experiment (data not shown). Figure 3 shows the double-reciprocal (Lineweaver−Burk) plots for TTLL7-catalyzed incorporation of glutamate into tubulin purified from adult mouse (AD) brain. We made six plots, since TTLL7 had three substrates (ATP, glutamate, and tubulin).

First, we plotted the changes in 1/*V* at different concentrations of ATP and glutamate at a fixed tubulin concentration, 17 μM, to determine the mode of binding between ATP and glutamate. Plots of 1/*V* versus 1/[ATP] at three different Glu

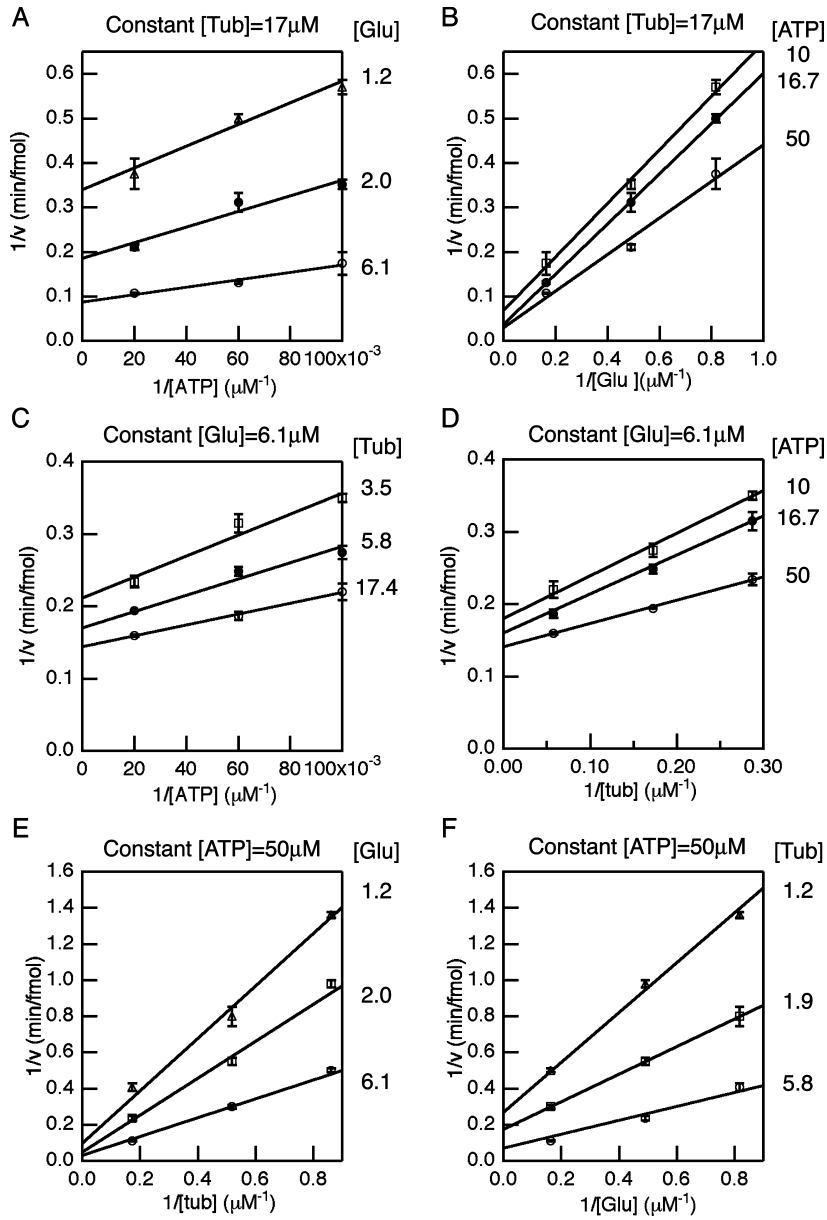

FIGURE 3: Dependence of polyglutamylase activity on substrate concentration which reveals that substrate binding to TTLL7 is not a ping-pong mechanism. (A) Plot of the reciprocal initial reaction velocity of TTLL7 vs the reciprocal of ATP concentration at various levels of [^{3}H]glutamate and at a fixed tubulin concentration (17 μM). [^{3}H]Glutamate concentrations were 6.1 (○), 2.0 (●), and 1.2 μM (△). (B) Plot of the reciprocal initial reaction velocity of TTLL7 vs [^{3}H]glutamate concentration at various levels of ATP and at a fixed tubulin concentration (17 μM). The ATP concentrations were 50 (○), 16.7 (●), and 10 μM (□). (C) Plot of the reciprocal initial reaction velocity of TTLL7 vs ATP concentration at various levels of tubulin (Tub) and at a fixed [^{3}H]glutamate concentration (6.1 μM). The tubulin concentrations were 17.4 (○), 5.8 (●), and 3.5 μM (□). (D) Plot of the reciprocal initial reaction velocity of TTLL7 vs tubulin concentration at various levels of ATP and at a fixed [^{3}H]glutamate concentration (6.1 μM). The ATP concentrations were 50 (○), 16.7 (●), and 10 μM (□). (E) Plot of the reciprocal initial reaction velocity of TTLL7 vs tubulin concentration at various levels of [^{3}H]glutamate and at a fixed ATP concentration (50 μM). [^{3}H]Glutamate concentrations were 6.1 (○), 2.0 (□), and 1.2 μM (△). (F) Plot of the reciprocal initial reaction velocity of TTLL7 vs [^{3}H]glutamate concentration at various levels of tubulin and at a constant ATP concentration (50 μM). The concentrations of tubulin were 5.8 (○), 1.9 (□), and 1.2 μM (△).

concentrations (1.2, 2.0, and 6.1 μM) were not parallel (Figure 3A). Plots of 1/V versus 1/[Glu] at three different ATP concentrations (10, 16.7, and 50 μM) were also not parallel (Figure 3B). We calculated the kinetic parameters at 17 μM adult mouse (AD) tubulin from secondary plots of the rate data: V_{max} = 5 nM/min, K_m(ATP) = 19 μM, and K_m(Glu) = 20 μM.

Next, we plotted the changes in 1/V at different ATP and tubulin concentrations at a fixed Glu concentration of 6.1 μM to determine the mode of binding between ATP and tubulin. The plots of 1/V versus 1/[ATP] at three different tubulin concentrations (3.5, 5.8, and 17.4 μM) (Figure 3C) and the plots of 1/V versus 1/[tubulin] at three different ATP concentrations (10, 16.7, and 50 μM) (Figure 3D) were not parallel. We calculated the kinetic parameters at 6.1 μM glutamate: V_{max} = 0.9 nM/min, K_m(ATP) = 7.5 μM, and K_m(tubulin) = 3.1 μM.

Finally, we plotted the changes in 1/V at different tubulin and Glu concentrations at a fixed ATP concentration of 50 μM to determine the mode of binding between tubulin and glutamate. The plots of 1/V versus 1/[tubulin] at three different Glu concentrations (1.2, 2.0, and 6.1 μM) (Figure

Table 1: Kinetic Parameters of the TTLL7 Enzyme for Glutamylation

		K_m(Glu) (μM)	K_m(ATP) (μM)	K_m(tubulin) (μM)	V_{max} (μM/min)
17 μM tubulin	AD	20.2	19.1	−	5.3×10^{-3}
	NB	19.6	26.5		1.4×10^{-2}
50 μM ATP	AD	5.4	−	21.8	7.5×10^{-3}
	NB	4.4		15.8	1.0×10^{-2}
6 μM Glu	AD	−	7.5	3.1	8.8×10^{-4}
	NB		16.0	6.7	1.0×10^{-3}
mean value	AD	12.8	13.3	12.5	4.6×10^{-3}
	NB	12.0	21.3	11.3	8.5×10^{-3}

3E) and the plots of 1/*V* versus 1/[Glu] at three different tubulin concentrations (1.2, 1.9, and 5.8 μM) (Figure 3F) were also not parallel. We calculated the kinetic parameters at 50 μM ATP: V_{max} = 7.5 nM/min, K_m(tub) = 21.8 μM, and K_m(Glu) = 5.4 μM.

We performed the same analyses for newborn mouse (NB) tubulin. The patterns of double-reciprocal plots for three substrates are the same as those of AD tubulin; all plots were nonparallel (data not shown). The nonparallel patterns of all the double-reciprocal plots demonstrate that TTLL7 binds to three substrates by a sequential, and not a ping-pong, mechanism (*37, 38*). The kinetic parameters, except for V_{max}, are almost equal between AD and NB tubulins (Table 1).

Seeking Effective Inhibitors for TTLL7 Activity. We sought out effective inhibitors to investigate the enzymatic reaction pathway of TTLL7 in more detail. To this end, we first tested the inhibition efficiency of several substances to find effective inhibitors for three substrates (Glu, ATP, and tubulin).

The efficacy of amino acids (L-Gln, L-Gly, L-His, L-Leu, L-Asp, and L-Tyr) as inhibitors to L-Glu was examined. The assay was performed under conditions where concentrations of the potential inhibitors (10 mM) were 1000-fold higher than that of [^{3}H]glutamate (~6 μM). L-Gln, L-His, and L-Asp exhibited insufficient inhibition, as they inhibited TTLL7 activity ~30−50% (Figure 4A). To find an inhibitor that was more effective, we tested glutamate-containing dipeptides, γGlu-Glu, γGlu-Leu, and γGlu-Cys. Of the peptides tested, γGlu-Glu most effectively (~80%) inhibited the TTLL7 activity (Figure 4B).

Next, we examined the inhibition effects of ADP, AMP, and AMP-PNP on ATP. These potential inhibitors, when used at a 600-fold higher concentration compared with the ATP concentration, almost completely inhibited the TTLL7 reaction (Figure 4C).

We finally sought out effective inhibitors for tubulin. We investigated C-terminal peptides with ~20 amino acid residues of class III or IV β-tubulins that are neuron specific β-tubulins (*39*) for their potencies in inhibiting the glutamylation of MTs by TTLL7 (Figure 4D). These peptides effectively (80%) inhibited the incorporation of [^{3}H]glutamate into tubulin at 30 mM, which was ~1000 times higher than that of tubulin.

Inhibitor Effects for Kinetics Reveal That TTLL7 Operates by a Random Sequential Pathway. We examined the inhibitor effects by using γGlu-Glu, AMP-PNP, and a class III β-tubulin peptide (Figure 5A−I). γGlu-Glu acted as a competitive inhibitor for glutamate as three regression lines intersected on the 1/*V* axis (Figure 5A) (*40*). In contrast, γGlu-Glu acted as a noncompetitive inhibitor for ATP and tubulin as the lines in panels B and C of Figure 5 did not cross on the 1/*V* axis (*40*). We calculated the inhibitor constants, K_I (Figure 5J), from the replot of 1/*V* versus [γGlu-Glu] (Dixon plot) (*41*): 1.1 mM for glutamate, 1.41 mM for ATP, and 0.29 mM for tubulin.

Similar results were obtained for the other inhibitors. AMP-PNP exhibited competitive inhibition for ATP (Figure 5E), whereas it acted as a noncompetitive inhibitor for glutamate (Figure 5D) and tubulin (Figure 5F). The calculated K_I values of AMP-PNP were 0.02 mM for ATP, 0.12 mM for glutamate, and 0.23 mM for tubulin. The C-terminal peptide of class III β-tubulin acted as a competitive inhibitor for tubulin (Figure 5I). By contrast, noncompetitive inhibitions were observed against glutamate (Figure 5G) and ATP (Figure 5H). The K_I values of the class III β-tubulin peptide were calculated as follows: 0.5 mM for tubulin, 1.06 mM for Glu, and 0.83 mM for ATP.

All the results of the kinetic analyses for inhibitors indicate that recombinant TTLL7 operates by the random sequential substrate binding mechanism for three substrates, glutamate, ATP, and MTs. This is a typical random sequential pathway that interconnects enzymes with various binary, ternary, and quaternary complexes (Figure 5K).

We finally calculated two inhibitor parameters, K_I and K_I', for noncompetitive inhibition from the inhibitor experiments. K_I is the first inhibitor parameter, and K_I' is the second inhibitor parameter (Figure 5J). The observed values are summarized in Table 2. K_I and K_I' of γGlu-Glu for ATP were almost identical: K_I = 1.41 mM, and K_I' = 1.39 mM. Similarly, K_I and K_I' of the β-tubulin III peptide for ATP were almost identical: K_I = 0.83 mM, and K_I' = 0.98 mM. In contrast, K_I and K_I' of γGlu-Glu for tubulin were drastically different: K_I = 0.29 mM, and K_I' = 5.98 mM.

DISCUSSION

In this report, we reveal the enzymatic properties of a mammalian β-tubulin-specific polyglutamylase, TTLL7, by a pure in vitro reaction system employing bacterially expressed recombinant protein. We obtained two novel findings. Of special note is the fact that recombinant TTLL7 exhibited significant initiation and elongation activities in the polyglutamylation on β-tubulin under the most optimal conditions. In addition, the substrate binding mechanism of TTLL7 was a random sequential pathway for three substrates (ATP, glutamate, and MTs).

We found optimal conditions for recombinant TTLL7. The substrate selectivity of TTLL7 depended on whether the tubulins were polymerized (Figure 1C). TTLL7 activity for depolymerized tubulin dimer decreases ~40% for MTs. This result is similar to that of polyglutamylase purified from mouse brain. The activity for depolymerized tubulin decreased to 25% for MTs at pH 8.7 (*22*). Furthermore, the specificity of polyglutamylation for β-tubulin of TTLL7 is lost on depolymerized tubulin, because of the decrease in the level of polyglutamylation for β-tubulin. Our finding suggests that TTLL7 recognizes a reactive glutamate site on β-tubulin on the basis of association with MTs. The preference of TTLL7 for polymerized tubulins highly contrasts to the case of TTL. TTL has high activity for the depolymerized tubulin dimer (*42, 43*). By V8 proteinase

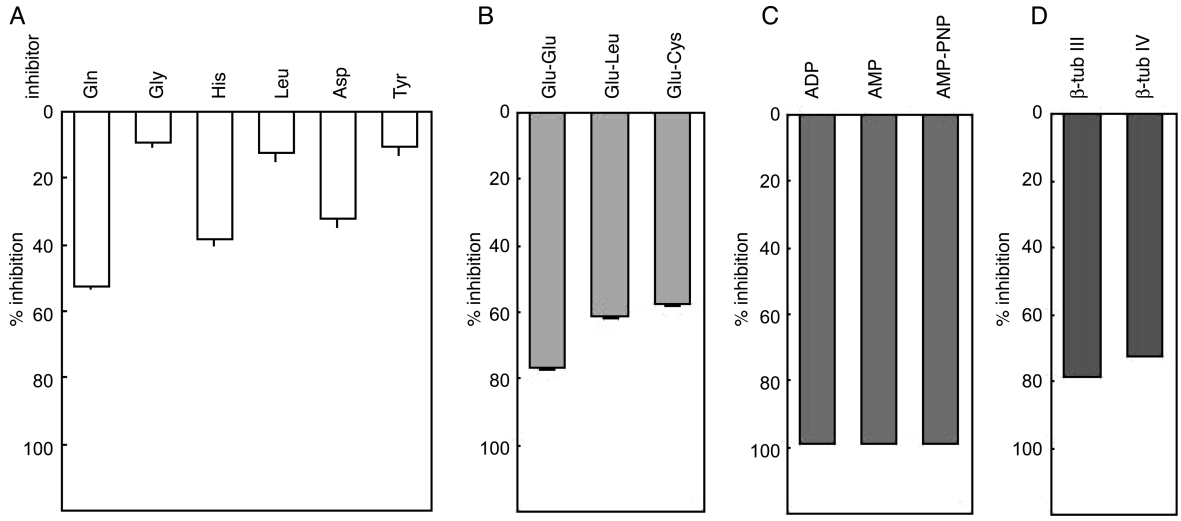

FIGURE 4: Inhibitory efficiency of several amino acid residues, glutamate peptides, ATP homologues, and β-tubulin C-terminal peptides. (A) Inhibitory effects for the reaction mixture of 6 μM glutamate, 50 μM ATP, and 16 μM tubulin: L-Gln (10 mM), L-Gly (10 mM), L-His (10 mM), L-Leu (10 mM), L-Asp (3 mM), and L-Tyr (0.2 mM). (B) γGlu-Glu (10 mM), γGlu-Leu (10 mM), and γGlu-Cys (10 mM). (C) ADP (30 mM), AMP (30 mM), and AMP-PNP (30 mM). (D) β-Tubulin C-terminal peptide classes III and IV.

digestion of TTL, it was reported that TTL is composed of two domains, one which interacts with the reactive α-tubulin C-terminus and the other which associates with the β-tubulin subunit of the dimer (*44*). The non-TTL domain present in TTLL7 might contain recognition sites for polymerized tubulins. In fact, the long non-TTL domain is essential for the enzymatic activity of TTLL7 (*28*).

Most interestingly, recombinant TTLL7 was able to elongate the polyglutamate chain by up to 16 glutamate residues in our experiments (Figure 2). The number of glutamates added on β-tubulin was twice as high as that observed in β-tubulin purified from adult brain (*30, 45*). Thus, TTLL7 per se has a strong elongase activity sufficient to polyglutamylate neuronal β-tubulins up to an endogenous level. Our conclusion clearly differs from that of an in vivo study concluding that TTLL7 dominantly performs as an initiase (*28*). The non-neuronal HeLa cells used in the other study (*28*) can possess strong reverse enzyme activities, as they endogenously exhibit little polyglutamylation (*8, 22*). Thus, in vivo, such a strong reverse enzyme activity might result in the apparent low efficiency of elongase activity. This idea can also explain why the level of polyglutamylation detected in our experiment was significantly higher than the in vivo glutamylation level detected in the brain. Glutamate-removing enzymes contained in the brain (*30*) could decrease the polyglutamylation level of β-tubulin in vivo.

We observed the enzyme kinetics of tubulin polyglutamylase for the first time (Figure 3). The mean values of the Michaelis constant for TTLL7 were as follows: K_m(ATP) = 13.3 or 21.3 μM, K_m(Glu) = 12.8 or 12.0 μM, and K_m(tubulin) = 12.5 or 11.3 μM for adult or newborn mouse MT, respectively (Table 1). The kinetic parameters are almost identical between AD and NB tubulin except for V_{max}. NB tubulin is almost composed of non-, mono-, and diglutamylated β-tubulin (Figure 2B). In contrast, AD tubulin is reported to include more glutamylated (up to nine) β-tubulin (*30*). Therefore, this difference in V_{max} between AD and NB tubulin indicates that initiation and/or the early step of elongation proceeded faster than the late step of elongation.

The K_m values of ATP and glutamate are significantly lower than the intracellular concentrations of ATP in the cerebral cortex (~3 mM) (*46*) and glutamate in brain tissue (~8 mM) (*47*). Thus, TTLL7 is likely to be saturated always with ATP and glutamate. In contrast, the K_m value of tubulin is close to a typical concentration of tubulin (subunit) in vivo, 1 mg/mL, i.e., 20 μM (*48*). This implies that the binding of TTLL7 to MTs determines the polyglutamylation activity in vivo. In addition, the K_m value of TTLL7 for tubulin is 10-fold higher than that of TTL (*43*). This difference might originate from the difference in substrate. TTLL7 can target all polymerized tubulins, while TTL targets a subpopulation of unpolymerized tubulins. Half of brain tubulin undergoes a removal of the penultimate glutamate residue, which is not subjected to tyrosination (*49, 50*). Thus, the smaller K_m(tubulin) value of TTL compared to that of TTLL7 could show that TTL efficiently catalyzes tyrosination in the presence of lower tubulin concentrations.

We identified a number of inhibitors of TTLL7. One of the inhibitors, γGlu-Glu, provides information regarding substrate usage by TTLL7. The obtained inhibitor constant of γGlu-Glu for glutamate, K_I(γGlu-Glu) (1.1 mM), is ~92 times larger than K_m(Glu) (12 μM). This value suggests that TTLL7 does not use the diglutamate peptide as a substrate during the polyglutamylase reaction.

We determined that the reaction mode of recombinant TTLL7 was a random sequential mechanism (Figure 5). Drastically different K_I and K_I' values, which are two inhibitor parameters for noncompetitive inhibition (Figure 5J), were obtained between γGlu-Glu and tubulin, or between the β-tubulin III peptide and glutamate (Table 2). In other combinations, there was little difference between the K_I and K_I' values (Table 2). The results indicate that glutamate and tubulin compete with each other in the enzyme reaction center, whereas ATP binds to TTLL7 in a manner independent of other substrates (*40*). This interpretation is in good agreement with the reported structure of the reaction center of the ADP-forming enzyme, which is highly homologous to TTLL proteins. In the ADP-forming enzyme, an ATP-binding pocket is separately placed from other substrate binding sites, whereas amino acid- or peptide-binding sites are adjacent (*25, 51*) (see S2 of the Supporting Information).

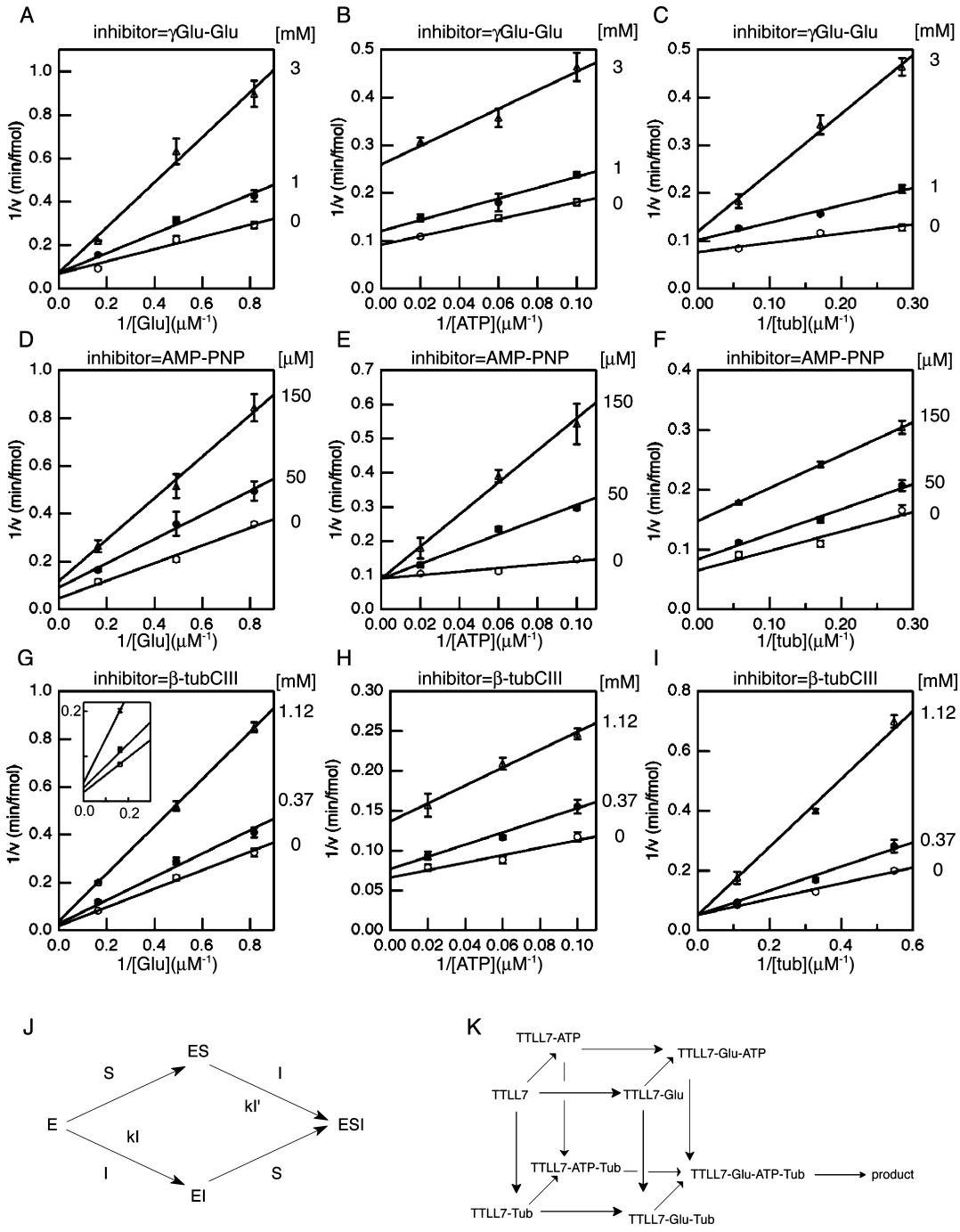

FIGURE 5: Kinetic studies of inhibition indicate that the substrate binding pathway is a random sequential pathway. (A−C) Inhibitory effects of the γGlu-Glu peptide. (A) Plot of the reciprocal initial reaction velocity of TTLL7 vs [^{3}H]glutamate concentration at various levels of γGlu-Glu peptide and at constant ATP (50 μM) and tubulin (18.3 μM) concentrations. The concentrations of γGlu-Glu in panels A−C were 0 (○), 1 (●), and 3 mM (△). (B) Plot of the reciprocal initial reaction velocity of TTLL7 vs ATP concentration at various levels of γGlu-Glu peptide and at constant [^{3}H]glutamate (6.1 μM) and tubulin (18.3 μM) concentrations. (C) Plot of the reciprocal initial reaction velocity of TTLL7 vs tubulin concentration at various levels of γGlu-Glu peptide and at constant [^{3}H]glutamate (6.1 μM) and ATP (50 μM) concentrations. (D−F) Inhibitory effects of AMP-PNP. (D) Plot of the reciprocal initial reaction velocity of TTLL7 vs ATP concentration at various levels of AMP-PNP and at constant [^{3}H]glutamate (6.1 μM) and tubulin (18.3 μM) concentrations. The concentrations of AMP-PNP in panels D−F were 0 (○), 50 (●), and 150 μM (△). (E) Plot of the reciprocal initial reaction velocity of TTLL7 vs [^{3}H]glutamate concentration at various levels of AMP-PNP and at constant ATP (50 μM) and tubulin (18.3 μM) concentrations. (F) Plot of the reciprocal initial reaction velocity of TTLL7 vs tubulin concentration at various levels of AMP-PNP and at constant [^{3}H]glutamate (6.1 μM) and ATP (50 μM) concentrations. (G−I) Inhibitory effects of the class III β-tubulin C-terminal peptide (β-tubCIII). (G) Plot of the reciprocal initial reaction velocity of TTLL7 vs tubulin concentration at various levels of β-tubCIII and at constant [^{3}H]glutamate (6.1 μM) and ATP (50 μM) concentrations. The concentrations of β-tubCIII in panels G−I were 0 (○), 0.37 (●), and 1.12 mM (△). The enlarged plot around the origin of panel G is inserted. (H) Plot of the reciprocal initial reaction velocity of TTLL7 vs [^{3}H]glutamate concentration at various levels of β-tubCIII and at constant ATP (50 μM) and tubulin (18.3 μM) concentrations. (I) Plot of the reciprocal initial reaction velocity of TTLL7 vs ATP concentration at various levels of β-tubCIII and at constant [^{3}H]glutamate (6.1 μM) and tubulin (18.3 μM) concentrations. (J) Scheme of noncompetitive inhibition, where E is enzyme, S is substrate, I is inhibitor, kI is first inhibition parameter, and kI′ is the second inhibition parameter. (K) Scheme of a random sequential pathway for three substrates (glutamate, ATP, and tubulin).

Table 2: Inhibitor Constants for the TTLL7 Enzymatic Reaction in Vitro

	γGlu-Glu			AMP-PNP			β-tubIII peptide		
	Glu	ATP	tubulin	Glu	ATP	tubulin	Glu	ATP	tubulin
K_I (mM)	1.1	1.41	0.29	0.12	0.02	0.22	1.06	0.83	0.5
K_I' (mM)	−	1.39	5.98	0.12	−	0.1	2.2	0.98	−

Our high-resolution two-dimensional PAGE and mass spectrometry revealed that TTLL7 per se was able to perform both initiation and elongation reactions (Figure 2). This "multi"-functional property of TTLL7 is highly contrasted to characteristics of other poly-modification enzymes, e.g., ubiquitin ligases and glycosylation enzymes. In ubiquitination, polyubiquitination is catalyzed by a stepwise reaction mediated by ubiquitin ligase complexes (E1−E3) (*52*). The C-terminal carboxyl group of a ubiquitin (Ub) is first ligated to the active cysteine of the E1 enzyme as an initiation. Subsequently, the Ub is transferred to the active cysteine in an E2 enzyme. The elongation of Ub to active lysine on Ub is catalyzed by E3 ligase (*53, 54*). In the case of glycosylation, each initiation and elongation step is catalyzed properly by different transferase enzymes (*55*). Thus, TTLL7, and possibly other polyglutamylase TTLLs, have enzymatically different features compared to those of other poly-modification-performing enzymes. Further investigations are needed to determine whether this idea can be applied to other polyglutamylases and polyglycylases.

In this research, we reported the enzymatic properties of a recombinant tubulin polyglutamylase, TTLL7. Several properties are different from those previously reported for polyglutamylase purified from mammalian tissues. Those differences might be caused by the contamination of inhibitors, enhancers, or deglutamylases in previously reported assays. Our pure in vitro reaction system clarified a complex enzymatic reaction like poly-modifications. The properties of TTLL7 are unique, even compared to those of other poly-modification-performing enzymes.

ACKNOWLEDGMENT

We thank Dr. B. Edde and Dr. C. Janke for providing monoclonal antibody GT335 and for their valuable suggestions. We thank the members of MITILS, especially Dr. Hatanaka, Dr. Taira, Ms. Yasutake, Ms. Miyaike, Ms. Ichinose, Mr. Satou, and Mr. Hatanaka for their technical assistance and advice.

SUPPORTING INFORMATION AVAILABLE

Structural analysis of the polyglutamylated C-terminal peptide of β-tubulin and MS^n spectra of the synthetic β-tubulin C-terminal peptides with or without extra glutamates and NB sample (S1) and sequence alignment between TTLL7 and ADP-forming enzymes and the X-ray structure of the substrate binding pocket of the ADP-forming enzyme (S2). This material is available free of charge via the Internet at http://pubs.acs.org.

REFERENCES

1. Setou, M., Hayasaka, T., and Yao, I. (2004) Axonal transport versus dendritic transport. *J. Neurobiol. 58*, 201–206.
2. Setou, M., Nakagawa, T., Seog, D., and Hirokawa, N. (2000) Kinesin superfamily motor protein KIF17 and mLin-10 in NMDA receptor-containing vesicle transport. *Science 288*, 1796–1802.
3. Setou, M., Seog, D., Tanaka, Y., Kanai, Y., Takei, Y., Kawagishi, M., and Hirokawa, N. (2002) Glutamate-receptor-interacting protein GRIP1 directly steers kinesin to dendrites. *Nature 417*, 83–87.
4. Ikegami, K., Robb, L., Taruishi, M., Takagi, H., Mukai, M., Shimma, S., Taira, S., Hatanaka, K., Morone, N., Yao, I., Campbell, P., Yuasa, S., Janke, C., MacGregor, G., and Setou, M. (2007) Loss of α-Tubulin Polyglutamylation in ROSA22 Mice is Associated with Abnormal Targeting of KIF1A and Modulated Synaptic Function. *Proc. Natl. Acad. Sci. U.S.A. 104*, 3213–3218.
5. Gagnon, C., White, D., Cosson, J., Huitorel, P., Edde, B., Desbruyeres, E., Paturle-Lafanechere, L., Multigner, L., Job, D., and Cibert, C. (1996) The polyglutamylated lateral chain of α-tubulin plays a key role in flagellar motility. *J. Cell Sci. 109*, 1545–1553.
6. Million, K., Larcher, J., Laoukili, J., Bourguignon, D., Marano, F., and Tournier, F. (1999) Polyglutamylation and polyglycylation of α- and β-tubulins during in vitro ciliated cell differentiation of human respiratory epithelial cells. *J. Cell Sci. 112*, 4357–4366.
7. Bobinnec, Y., Moudjou, M., Fouquet, J., Desbruyeres, E., Edde, B., and Bornens, M. (1998) Glutamylation of centriole and cytoplasmic tubulin in proliferating non-neuronal cells. *Cell Motil. Cytoskeleton 39*, 223–232.
8. Regnard, C., Desbruyeres, E., Denoulet, P., and Edde, B. (1999) Tubulin polyglutamylase: Isozymic variants and regulation during the cell cycle in HeLa cells. *J. Cell Sci. 112*, 4281–4289.
9. Westermann, S., and Weber, K. (2003) Post-translational modifications regulate microtubule function. *Nat. Rev. 4*, 938–947.
10. Reed, N., Cai, D., Blasius, T., Jih, G., Meyhofer, E., Gaertig, J., and Verhey, K. (2006) Microtubule acetylation promotes kinesin-1 binding and transport. *Curr. Biol. 16*, 2166–2172.
11. Eipper, B. (1974) Properties of rat brain tubulin. *J. Biol. Chem. 249*, 1407–1416.
12. Gard, D., and Kirschner, M. (1985) A polymer-dependent increase in phosphorylation of β-tubulin accompanies differentiation of a mouse neuroblastoma cell line. *J. Cell Biol. 100*, 764–774.
13. Gurland, G., and Gundersen, G. (1995) Stable, detyrosinated microtubules function to localize vimentin intermediate filaments in fibroblasts. *J. Cell Biol. 131*, 1275–1290.
14. Dunn, S., Morrison, E., Liverpool, T., Molina-Paris, C., Cross, R., Alonso, M., and Peckham, M. (2008) Differential trafficking of Kif5c on tyrosinated and detyrosinated microtubules in live cells. *J. Cell Sci. 121*, 1085–1095.
15. Thazhath, R., Liu, C., and Gaertig, J. (2002) Polyglycylation domain of β-tubulin maintains axonemal architecture and affects cytokinesis in *Tetrahymena*. *Nat. Cell Biol. 4*, 256–259.
16. Larcher, J., Boucher, D., Lazereg, S., Gros, F., and Denoulet, P. (1996) Interaction of kinesin motor domains with α- and β-tubulin subunits at a τ-independent binding site. Regulation by polyglutamylation. *J. Biol. Chem. 271*, 22117–22124.
17. Bonnet, C., Boucher, D., Lazereg, S., Pedrotti, B., Islam, K., Denoulet, P., and Larcher, J. (2001) Differential binding regulation of microtubule-associated proteins MAP1A, MAP1B, and MAP2 by tubulin polyglutamylation. *J. Biol. Chem. 276*, 12839–12848.
18. Ikegami, K., Mukai, M., Tsuchida, J., Heier, R., MacGregor, G., and Setou, M. (2006) TTLL7 is a mammalian β-tubulin polyglutamylase required for growth of MAP2-positive neurites. *J. Biol. Chem. 281*, 30707–30716.
19. Barra, H., Arce, C., Rodriguez, J., and Caputto, R. (1974) Some common properties of the protein that incorporates tyrosine as a single unit and the microtubule proteins. *Biochem. Biophys. Res. Commun. 60*, 1384–1390.
20. Argarana, C., Barra, H., and Caputto, R. (1978) Release of [^{14}C]tyrosine from tubulinyl-[^{14}C]tyrosine by brain extract. Separation of a carboxypeptidase from tubulin-tyrosine ligase. *Mol. Cell. Biochem. 19*, 17–21.
21. Gundersen, G., Kalnoski, M., and Bulinski, J. (1984) Distinct populations of microtubules: Tyrosinated and nontyrosinated α-tubulin are distributed differently in vivo. *Cell 38*, 779–789.
22. Regnard, C., Audebert, S., Desbruyeres, E., Denoulet, P., and Edde, B. (1998) Tubulin Polyglutamylase: Partial Purification and Enzymatic Properties. *Biochemistry 37*, 8395–8404.
23. Regnard, C., Fesquet, D., Janke, C., Boucher, D., Desbruyeres, E., Koulakoff, A., Insina, C., Travo, P., and Edde, B. (2003) Characterisation of PGs1, a subunit of a protein complex co-purifying with tubulin polyglutamylase. *J. Cell Sci. 116*, 4181–4190.

24. Janke, C., Rogowski, K., Wloga, D., Regnard, C., Kajava, A., Strub, J.-M., Temurak, N., van Dijk, J., Boucher, D., van Dorsselaer, A., Suryavanshi, S., Gaertig, J., and Edde, B. (2005) Tubulin polyglutamylase enzymes are members of the TTL domain protein family. *Science 308*, 1758–1762.
25. Fan, C., Moews, P., Walsh, C., and Knox, J. (1994) Vancomycin resistance: Structure of D-alanine:D-alanine ligase at 2.3 Å resolution. *Science 266*, 439–443.
26. Dideberg, O., and Bertrand, J. (1998) Tubulin tyrosine ligase: A shared fold with the glutathione synthetase ADP-forming family. *Trends Biochem. Sci. 23*, 57–58.
27. Galperin, M., and Koonin, E. (1997) A diverse superfamily of enzymes with ATP-dependent carboxylate-amin/thiol ligase activity. *Protein Sci. 6*, 2639–2643.
28. Van Dijk, J., Rogowski, K., Miro, J., Lacroix, B., Edde, B., and Janke, C. (2007) A Targeted Multienzyme Mechanism for Selective Microtubule Polyglutamylation. *Mol. Cell 26*, 437–448.
29. Ikegami, K., Horigome, D., Mukai, M., Livnat, I., MacGregor, G., and Setou, M. (2008) TTLL10 is a protein polyglycylase that can modify nucleosome assembly protein 1. *FEBS Lett. 582*, 1129–1134.
30. Audebert, S., Koulakoff, A., Berwald-Netter, Y., Gros, F., Denoulet, P., and Edde, B. (1994) Developmental regulation of polyglutamylated α- and β-tubulin in mouse brain neurons. *J. Cell Sci. 107*, 2313–2322.
31. Wolff, A., Houdayer, M., Chillet, D., de Nechaud, B., and Denoulet, P. (1994) Structure of the polyglutamyl chain of tubulin: Occurrence of α and γ linkages between glutamyl units revealed by monoreactive polyclonal antibodies. *Biol. Cell 81*, 11–16.
32. Sugiura, Y., Shimma, S., and Setou, M. (2006) Two-step matrix application technique to improve ionization efficiency for matrix-assisted laser desorption/ionization in imaging mass spectrometry. *Anal. Chem. 78*, 8227–8235.
33. Taira, S., Sugiura, Y., Moritake, S., Shimma, S., Ichiyanagi, Y., and Setou, M. (2008) Nanoparticle-assisted laser desorption/ionization based mass imaging with cellular resolution. *Anal. Chem. 80*, 4761–4766.
34. Redeker, V., Le Caer, J., Rossier, J., and Prome, J. (1991) Structure of the polyglutamyl side chain posttranslationally added to α-tubulin. *J. Biol. Chem. 266*, 23461–23466.
35. Westermann, S., Schneider, A., Horn, E., and Weber, K. (1999) Isolation of tubulin polyglutamylase from *Crithidia*: Binding to microtubules and tubulin, and glutamylation of mammalian brain α- and β-tubulins. *J. Cell Sci. 112*, 2185–2193.
36. Alexander, J., Hunt, D., Lee, M., Shabanowitz, J., Michel, H., Berlin, S., MacDonald, T., Sundberg, R., Rebhun, L., and Frankfurter, A. (1991) Characterization of posttranslational modifications in neuron-specific class III β-tubulin by mass spectrometry. *Proc. Natl. Acad. Sci. U.S.A. 88*, 4685–4689.
37. Cleland, W. (1963) The kinetics of enzyme-catalyzed reactions with two or more substrates or products. I. Nomenclature and rate equations. *Biochim. Biophys. Acta 67*, 104–137.
38. Cleland, W. (1979) Statistical analysis of enzyme kinetic data. *Methods Enzymol. 63*, 103–138.
39. Lee, M., Tuttle, J., Rebhun, L., Cleveland, D., and Frankfurter, A. (1990) The expression and posttranslational modification of a neuron-specific β-tubulin isotype during chick embryogenesis. *Cell Motil. Cytoskeleton 17*, 118–132.
40. Cleland, W. (1963) The kinetics of enzyme-catalyzed reactions with two or more substrates or products. II. Inhibition: Nomenclature and theory. *Biochim. Biophys. Acta 67*, 173–187.
41. Dixon, M., and Webb, E. C. (1964) *Enzymes*, 2nd ed., Academic Press, New York.
42. Raybin, D., and Flavin, M. (1977) Enzyme which specifically adds tyrosine to the α chain of tubulin. *Biochemistry 16*, 2189–2194.
43. Deans, N., Allison, R., and Purich, D. (1992) Steady-state kinetics mechanism of bovine brain tubulin: Tyrosine ligase. *Biochem. J. 286*, 243–251.
44. Wehland, J., and Weber, K. (1987) Tubulin-tyrosine ligase has a binding site on β-tubulin: A two-domain structure of the enzyme. *J. Cell Biol. 104*, 1059–1067.
45. Rudiger, A., Rudiger, M., Weber, K., and Schomburg, D. (1995) Characterization of Posttranslational Modifications of Brain Tubulin by Matrix-Assisted Laser Desorption/Ionization Mass Spectrometry: Direct One-Step Analysis of a Limited Subtilisin Digest. *Anal. Biochem. 224*, 532–537.
46. Bachelard, H. (1971) Allosteric activation of brain hexokinase by magnesium ions and by magnesium ion: Adenosine triphosphate complex. *Biochem. J. 125*, 249–254.
47. Blosser, J., and Wells, W. (1972) Studies on amino acid levels and protein metabolism in the brains of galactose-intoxicated chicks. *J. Neurochem. 19*, 69–79.
48. Soltys, B., and Borisy, G. (1985) Polymerization of tubulin in vivo: Direct evidence for assembly onto microtubule ends and from centrosomes. *J. Cell Biol. 100*, 1682–1689.
49. Paturle-Lafanechère, L., Eddé, B., Denoulet, P., Van Dorsselaer, A., Mazarguil, H., Le Caer, J., Wehland, J., and Job, D. (1991) Characterization of a major brain tubulin variant which cannot be tyrosinated. *Biochemistry 30*, 10523–10528.
50. Rudiger, M., Wehland, J., and Weber, K. (1994) The carboxy-terminal peptide of detyrosinated α-tubulin provides a minimal system to study the substrate specificity of tubulin-tyrosine ligase. *Eur. J. Biochem. 220*, 309–320.
51. Yamaguchi, H., Kato, H., Hata, Y., Nishioka, T., Kimura, A., Oda, J., and Katsube, Y. (1993) Three-dimensional structure of the glutathione synthetase from *Escherichia coli* B at 2.0 Å resolution. *J. Mol. Biol. 229*, 1083–1100.
52. Scheffner, M., Nuber, U., and Huibregtse, J. (1995) Protein ubiquitination involving an E1-E2-E3 enzyme ubiquitin thioester cascade. *Nature 373*, 81–83.
53. Weissman, A. (2001) Themes and variations on ubiquitylation. *Nat. Rev. Mol. Cell Biol. 2*, 169–178.
54. Pickart, C. (2001) Mechanisms underlying ubiquitination. *Annu. Rev. Biochem. 70*, 503–533.
55. Kornfeld, R., and Kornfeld, S. (1985) Assembly of asparagine-linked oligosaccharides. *Annu. Rev. Biochem. 54*, 631–664.

BI802047Y